Dynamics of activity fronts in a continuum mean field model of cortex

Helmut Schmidt[1], Ingo Bojak[2,†] and Stephen Coombes[1]

[1]Institute of Neuroscience, School of Mathematical Sciences, University of Nottingham, Nottingham NG7 2RD, United Kingdom. [2]Donders Institute, Centre for Neuroscience, Radboud University Nijmegen Medical Centre, The Netherlands. [†]Presenting.

Donders Institute
for brain, cognition and behaviour

Introduction

The functional organization of cortex appears to be roughly columnar, with the laminar substructure of each column organizing its microcircuitry. These columns tessellate the two-dimensional cortical sheet with high density, e.g., 2,000 cm^2 of human cortex contain 10^5 to 10^6 macrocolumns, comprising about 10^5 neurons each. Continuum mean field models (cMFMs) describe the mean activity of such columns by approximating the cortical sheet as continuous excitable medium [1,2]. cMFMs can generate rich patterns of emergent spatiotemporal activity [3]. This has been used to understand phenomena from visual hallucinations to the generation of EEG and fMRI BOLD signals [4,5]. Pattern boundaries are here defined as the interface between low and high states of average neural activity.

cMFMs support travelling patterns as well as the formation of intricate structures. Here we derive equations of motion for the pattern boundaries of a simple cMFM, showing that their normal velocities can be computed from boundary integrals. The solutions of these exact, but dimensionally reduced, equations for activity fronts are in excellent numerical agreement with the full nonlinear integral equation. A linear stability analysis of the dynamics of the interfaces allows us to understand mechanisms of pattern formation arising from instabilities of spots, fronts and stripes. We further test these results against partial differential equations (PDEs) equivalent to the original integral equation [6], and perform numerical simulations on a sizable cortical sheet to study how more realistic firing rates (computed with sigmoidal functions instead of Heaviside steps) influence the dynamics of activity fronts.

Integral equation, equivalent PDE set and bump solution

We use here a bare-bones cMFM consisting of a single neuronal population with local excitation and distal inhibition, mimicking the behaviour of interacting excitatory and inhibitory neural subpopulations. This so-called Mexican hat connectivity is now known to underlie the generation of both spatially periodic and spatially localized structures; the latter have been hypothetically linked to working memory (the temporary storage of information within the brain).

Neural activity $u\left(\vec{r},t\right)$ with $\vec{r}=(r,\theta)$ and $r,t\in\mathbb{R}^+,\ \theta\in[0,2\pi)$ is governed by

$$u(\vec{r},t)=\int_{\mathbb{R}^2}d\vec{r}\,'\,w\left(\vec{r}-\vec{r}\,'\right)\int_0^t dt'\,\eta(t')f\left[u\left(\vec{r}\,',t-t'\right)\right]$$

with the following biologically motivated but simplistic definitions:

$$f(u)\equiv\begin{cases}\sigma>0: & 1/\left[1+e^{-(u-h)/\sigma}\right]\\ \sigma=0: & \Theta(u-h)\end{cases}$$ a function that converts activity into firing rate,

$\eta\left(t\right)\equiv\alpha e^{-\alpha t}\Theta(t)$ a synaptic filter, and finally also a synaptic connectivity footprint

$$w\left(\vec{r}\right)\equiv E(r)-\frac{1}{\gamma}E\left(\beta r\right)\qquad\text{where}\qquad E(r)\equiv\frac{2}{3\pi}\left[\mathrm{K}_0(r)-\mathrm{K}_0(2r)\right]\simeq\frac{1}{2\pi}e^{-r}.$$

The synaptic footprint is balanced $\int_{\mathbb{R}^2}d\vec{r}\,w\left(\vec{r}\right)=0$ if $\gamma=1/\beta^2$.

For the exponential synapse, the following integro-differential form arises

$$\frac{1}{\alpha}\frac{\partial u}{\partial t}=-u(\vec{r},t)+\underbrace{\int_{\mathbb{R}^2}d\vec{r}\,'\,w\left(\vec{r}-\vec{r}\,'\right)f\left[u\left(\vec{r}\,',t\right)\right]}_{\mathcal{F}^2:\ \frac{4}{3}\left\{\psi_1\left(\vec{k},t\right)-\psi_2\left(\vec{k},t\right)-\frac{1}{\gamma}\left[\psi_\beta\left(\vec{k},t\right)-\psi_{2\beta}\left(\vec{k},t\right)\right]\right\}}$$

where the 2D-Fourier transform ($\mathcal{F}^2\triangleq\mathcal{H}$, Hankel transform, if radially symmetric) is calculated using $\mathcal{H}\left[\mathrm{K}_0(pr)\right]=\frac{1}{p^2+k^2}$ and $\psi_p\left(\vec{k},t\right)\equiv\frac{1}{p^2+k^2}f\left[u\left(\vec{k},t\right)\right]$. Thus one finds the equivalent PDE set

$$\frac{1}{\alpha}\frac{\partial u}{\partial t}=-u(\vec{r},t)+\frac{4}{3}\left\{\psi_1\left(\vec{r},t\right)-\psi_2\left(\vec{r},t\right)-\frac{1}{\gamma}\left[\psi_\beta\left(\vec{r},t\right)-\psi_{2\beta}\left(\vec{r},t\right)\right]\right\}$$

$$\left(p^2-\nabla^2\right)\psi_p\left(\vec{r},t\right)=f\left[u\left(\vec{r},t\right)\right]$$

For the Heaviside firing rate, we can find a time-invariant, radially symmetric bump solution:

$$f\left[u^*\left(r\right)\right]=\Theta(R-r)\ \Rightarrow\ \psi_p^R\left(r\right)=\frac{R}{p}\cdot\begin{cases}r<R: & \frac{1}{pR}-\mathrm{I}_0(pr)\mathrm{K}_1(pR)\\ r\geq R: & \mathrm{I}_1(pR)\mathrm{K}_0(pr)\end{cases}$$

$$u^*\left(r\right)=\frac{4}{3}\left\{\psi_1^R(r)-\psi_2^R(r)-\frac{1}{\gamma}\left[\psi_\beta^R(r)-\psi_{2\beta}^R(r)\right]\right\}\ ,\quad u^*\left(R\right)=h$$

Next we will investigate the stability of this bump solution, which serves as our initial state.

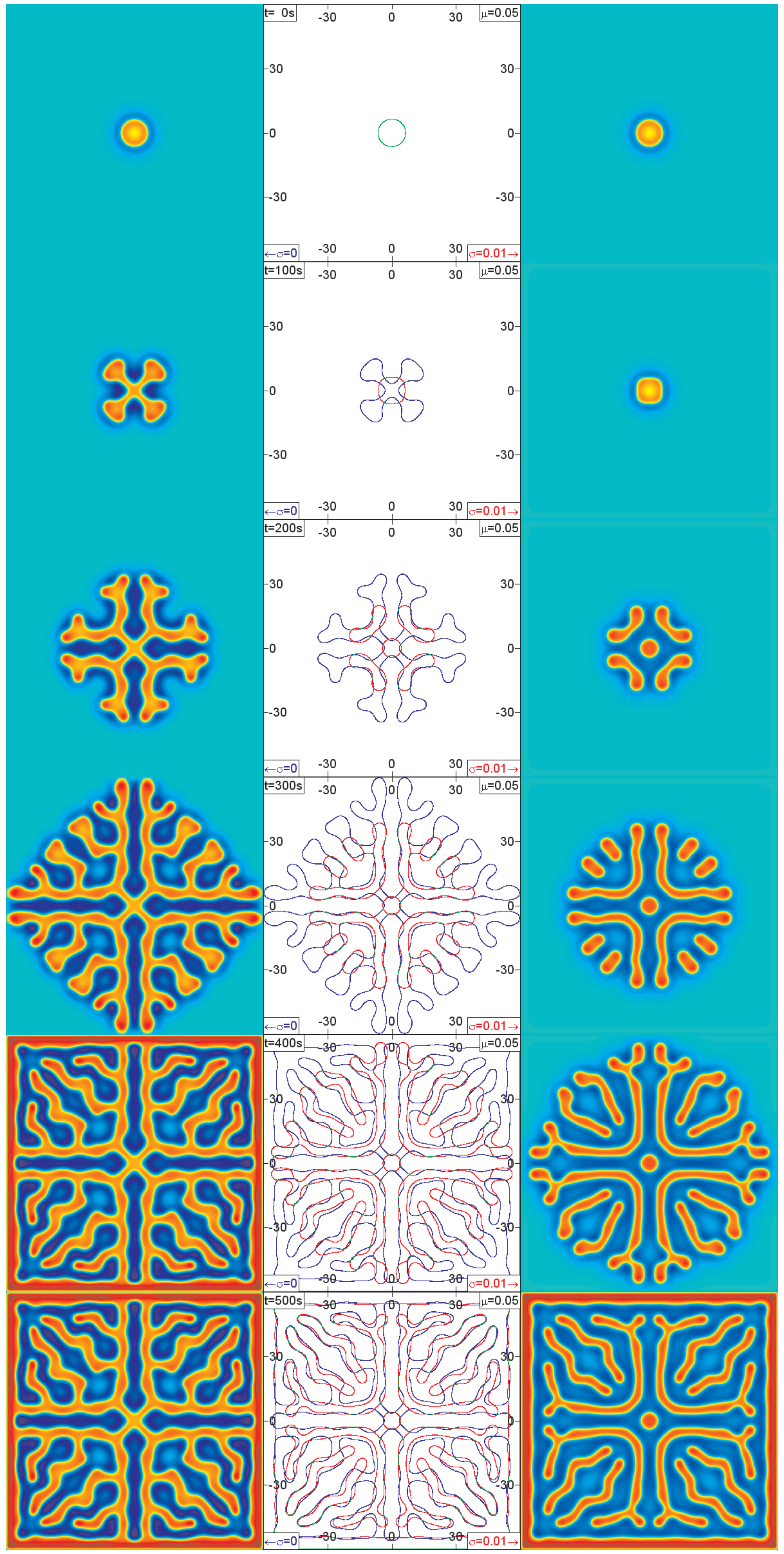

Stability analysis

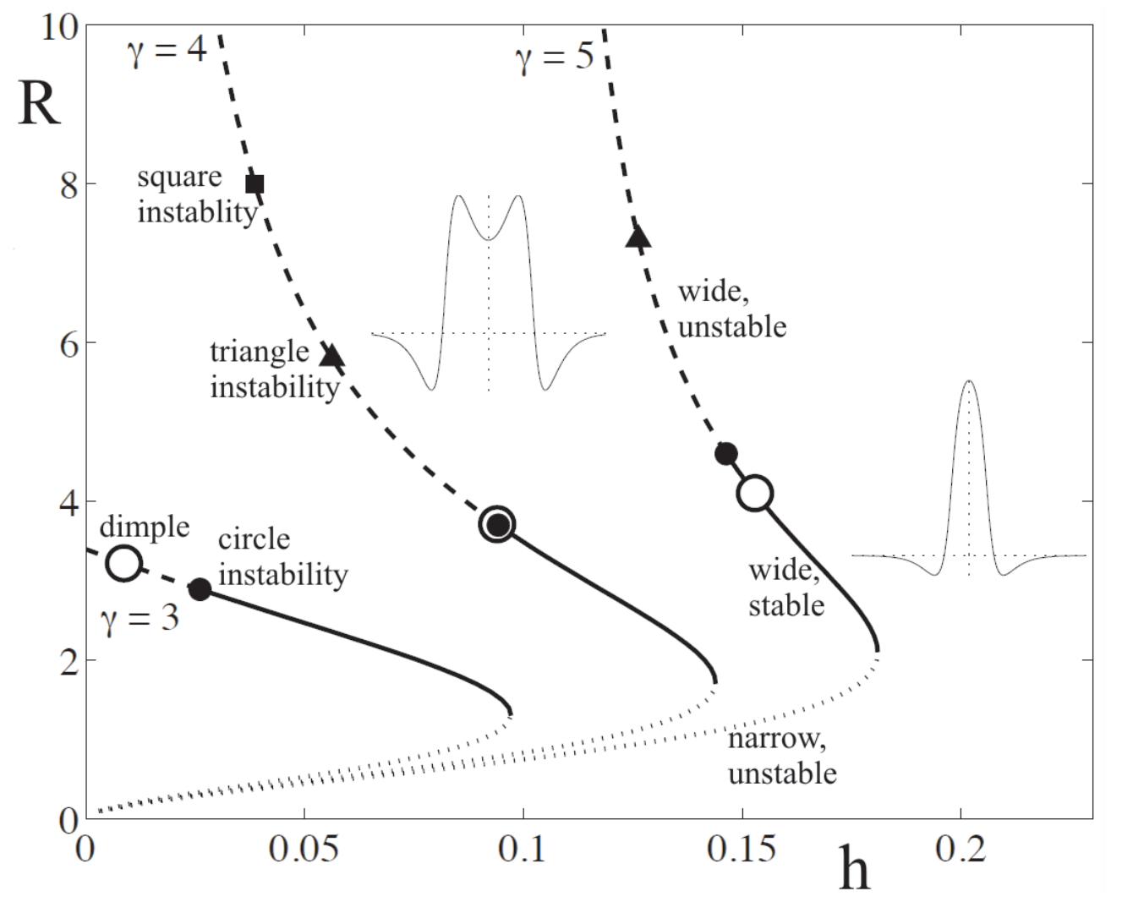

For bumps, one can find the discrete eigenvalue spectrum from the following Evans functions [7]:

$$\mathcal{E}_m(\lambda)\equiv\mathcal{L}[\eta](\lambda)^{-1}-\mu_m=0$$

$$\mu_m=\frac{2R}{|u^{*\prime}(R)|}\int_0^{2\pi}d\theta\,w(2R\sin\theta)\cos(2m\theta)$$

with Laplace transform $\mathcal{L}$. Stability requires then

$$\forall\ m\in\mathbb{Z}:\ \ \mathrm{Re}\left(\lambda_m\right)<0$$

otherwise the bump decays with m-fold symmetry.

Interface dynamics

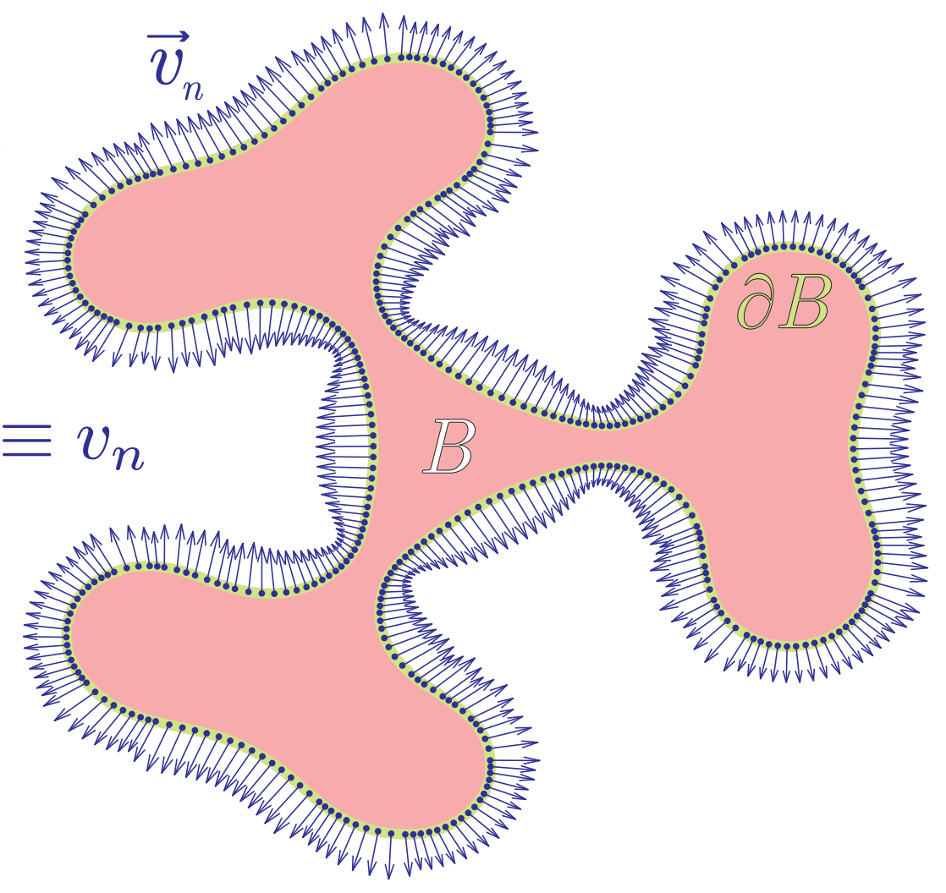

In the Heaviside case, consider some area (e.g., the bump solution) completely over threshold. One can then derive the normal velocities of the threshold boundary [8]:

$$\partial B:\ \ u\equiv u\left(\vec{r},t\right)|_{\vec{r}=\vec{R}}=h\ ,\quad\Rsh\quad\frac{\partial u/\partial t}{|\nabla u|}=\vec{n}\cdot\frac{\partial\vec{R}}{\partial t}\equiv v_n$$

$$\frac{du}{dt}=0=\nabla u\cdot\vec{R}_t+u_t=-\left|\nabla u\right|\vec{n}\cdot\vec{R}_t+u_t$$

We now show that the entire firing rate dynamics can be computed by evolving this interface alone.

The integro-differential form can under these circumstances be written as

$$\frac{1}{\alpha}u_t\left(\vec{r},t\right)=-u\left(\vec{r},t\right)+\sum_{i=1}^4c_i\int_B d\vec{r}\,'\,\mathrm{K}_0\left(\zeta_i\left|\vec{r}-\vec{r}\,'\right|\right)$$

Computing this restricted to the boundary yields the numerator of the normal velocities:

$$\frac{1}{\alpha}u_t=-\,h+\sum_{i=1}^4c_i\int_B d\vec{r}\,'\,\mathrm{K}_0\left(\zeta_i\left|\vec{R}-\vec{r}\,'\right|\right)$$

$$=-\,h+\sum_{i=1}^4\frac{c_i}{\zeta_i}\left[\frac{1}{\zeta_i}-\int_{\partial B}ds\,\vec{n}\cdot\frac{\vec{R}-\vec{R}(s)}{\left|\vec{R}-\vec{R}(s)\right|}\mathrm{K}_1\left(\zeta_i\left|\vec{R}-\vec{R}(s)\right|\right)\right]$$

For the denominator, we derive a transient equation on the interface by taking the gradient:

$$\frac{1}{\alpha}\left(\nabla_ru\right)_t\left(\vec{r},t\right)=-\,\nabla_ru(\vec{r},t)+\sum_{i=1}^4c_i\nabla_r\int_B d\vec{r}\,'\,\mathrm{K}_0\left(\zeta_i\left|\vec{r}-\vec{r}\,'\right|\right)$$

$$=-\,\nabla_ru(\vec{r},t)-\sum_{i=1}^4c_i\int_{\partial B}ds\,\vec{n}\,\mathrm{K}_0\left(\zeta_i\left|\vec{r}-\vec{R}(s)\right|\right)$$

$$\frac{1}{\alpha}\left(\nabla_ru\right)_t=-\nabla_ru-\sum_{i=1}^4c_i\int_{\partial B}ds\,\vec{n}\,\mathrm{K}_0\left(\zeta_i\left|\vec{R}-\vec{R}(s)\right|\right)$$

This allows evolving activity fronts from a chosen initial state. Predictions can be compared with direct simulations of the equivalent PDEs, and are in excellent agreement (see large figure).

Conclusions

On the cortical sheet, two-dimensional patterns can be defined by boundaries between high and low activity, and their dynamics can be specified by tracking the evolution of these interfaces. Using a simple cMFM, we have shown that one can faithfully describe the motion of activity fronts with equations of reduced complexity. This improves our ability to study pattern formation and suggests more generally that modelling the interfaces of patterns, rather than the patterns themselves, may lead to novel, efficient descriptions of brain activity.

References

[1] Coombes S (2010) *Large-scale neural dynamics: Simple and complex*. NeuroImage 52: 731-739.
[2] Deco GR, Jirsa VK, Robinson PA, Breakspear M, Friston KJ (2008) *The dynamic brain: From spiking neurons to neural masses and cortical fields.* PLoS Comput Biol 4: e1000092.
[3] Coombes S, Venkov NA, Shiau L, Bojak I, Liley DTJ, Laing CR (2007) *Modeling electrocortical activity through improved local approximations of integral neural field equations.* Phys Rev E 76: 051901.
[4] Bressloff PC, Cowan JD, Golubitsky M, Thomas PJ, Wiener MC (2001) *Geometric visual hallucinations, Euclidean symmetry and the functional architecture of striate cortex*. Philos Trans R Soc Lond B 356: 299-330.
[5] Bojak I, Oostendorp TF, Reid AT, Kötter R (2010) *Connecting mean field models of neural activity to EEG and fMRI data*. Brain Topogr 23: 139-149.
[6] Bojak I, Liley DTJ (2010) *Axonal velocity distributions in neural field equations.* PLoS Comput Biol 6: e1000653.
[7] Owen MR, Laing CR, Coombes S (2007) *Bumps and rings in a two-dimensional neural field: Splitting and rotational instabilities*. New J Phys 9: 378.
[8] Goldstein RE, Muraki DJ, Petrich DM (1996) *Interface proliferation and the growth of labyrinths in a reaction-diffusion system*. Phys Rev E 53: 3933-3957.

Donders Institute
for Brain, Cognition and Behaviour